Computers and Concrete, *Vol. 22, No. 5 (2018) 469-479*
DOI: https://doi.org/10.12989/cac.2018.22.5.469

Simulating the influence of pore shape on the Brazilian tensile strength of concrete specimens using PFC2D

Hadi Haeri[1], Vahab Sarfarazi[2a], Zheming Zhu[*1] and Mohammad Fatehi Marji[3b]

[1]*MOE Key Laboratory of Deep Underground Science and Engineering, School of Architecture and Environment, Sichuan University, Chengdu 610065, China*
[2]*Department of Mining Engineering, Hamedan University of Technology, Hamedan, Iran*
[3]*Department of Mining Engineering, Yazd University, Yazd, Iran*

(Received August 26, 2018, Revised November 14, 2018, Accepted November 15, 2018)

Abstract. The Brazilian tensile strength of concrete samples is a key parameter in fracture mechanics since it may significantly change the quality of concrete materials and their mechanical behaviors. It is well known that porosity is one of the most often used physical indices to predict concrete mechanical properties. In the present work the influence of porosity shape on concrete tensile strength characteristics is studied, using a bonded particle model. Firstly numerical model was calibrated by Brazilian experimental results and uniaxial test out puts. Secondly, Brazilian models consisting various pore shapes were simulated and numerically tested at a constant speed of 0.016 mm/s. The results show that pore shape has important effects on the failure pattern. It is shown that the pore shape may play an important role in the cracks initiation and propagation during the loading process which in turn influence on the tensile strength of the concrete samples. It has also been shown that the pore size mainly affects the ratio of uniaxial compressive strength to that of the tensile one in the simulated material samples.

Keywords: Brazilian tensile strength; pore shape effect; simulation by PFC2D; concrete specimens

1. Introduction

The porous concrete samples usually contain discontinuities which are mostly in form of micro cracks and pores. Therefore, the physical properties of these material samples may be affected by the existence and shape of these pores. it has been found by many researchers that with porosity increasing, the concretes mechanical properties and their permeability's (e.g., Al-Harthi *et al*. 1999, Chang *et al*. 2006, Zhu *et al*. 2011, Baud *et al*. 2014, Schaefer *et al*. 2015, Chang *et al*. 2006, Bourbié and Zinszner 1985, Farquharson *et al*. 2015). Most of these studies stated that the porosity may not significantly control the hydro-mechanical properties of rock like materials but the voids geometry within the structure of the concretes or rocks may drastically affect the mechanical properties of these materials such as their uniaxial tensile strengths (e.g., Chang *et al*. 2006, Farquharson *et al*. 2015).

A variety of numerical methods have been developed to study the mechanical behavior of rocks and concretes such as the domain methods (i.e., the finite element methods and the finite element methods) and the boundary methods such as the direct and indirect boundary element methods.

The higher order displacement discontinuity method which is a version of indirect boundary element method have also been developed and used in recent years to study the mechanical behavior and failure process and fracturing pattern of rocks and rock like materials such as concretes which are of importance in many geo-mechanical engineering applications in various fields of engineering such as mining, civil, petroleum geological and environmental (Marji *et al*. 2007, Hosseini_Nasab and Marji 2007, Marji 2014). The micro cracks and pores are usually assumed as elliptical voids within the texture of the rock or concrete samples. These discontinuities are considered to have different ratios of the minor to major axes of the ellipses. This ratio is unity for the perfectly spherical pores and can be as low as 10-3 to 10-5 for the micro cracks (Simmons and Richter 1976). It has been visualized by *X*-ray micro-computed tomography (μCT) that a wide variety of pores and micro cracks shapes can be observed in the porous rocks and concretes samples (e.g., Ji *et al*. 2012, Rozenbaum and Rolland du Roscat 2014, Ji *et al*. 2015, Schmitt *et al*. 2016, Luquot *et al*. 2016, Bubeck *et al*. 2017).

Some numerical models (in two and three dimensional spaces) have also been developed to study the effects of micro cracks and pores on the micro and macro mechanical properties of the porous rocks and concretes (e.g., Ashby and Sammis 1990, sarfarazi 2016a, b, haeri 2016 a, b) and circular pores (e.g., Sammis and Ashby 1986, Wu *et al*. 2010, Heap *et al*. 2014, Mobasher *et al*. 2014, Noel and Soudki 2014, Haeri *et al*. 2014, Pan *et al*. 2014, Oliveira and Leonel 2014, Tiang *et al*. 2015, Haeri 2015, Haeri *et al*. 2015a, b, c, Lee and Chang 2015, Kequan and Zhoudao 2015, Liu *et al*. 2015, Yaylac 2016, Fan *et al*. 2016, Li *et al*. 2016, Sardemir 2016, Wasantha *et al*. 2015, Sarfarazi *et al*.

∗Corresponding author, Professor
E-mail: zhemingzhu@hotmail.com
[a]Assistant Professor
[b]Associate Professor

ISSN: 1598-8198 (Print), 1598-818X (Online)

2016, Haeri *et al*. 2016a, b, c, Haeri and Sarfarazi 2016, Rajabi 2016, Mohammad 2016, Shuraim 2016, Wang *et al*. 2016, 2017, Wang *et al*. 2016a, Zhang *et al*. 2018, Zhou *et al*. 2018, Ma *et al*. 2017a, b, Khodayar and Nejati 2018, Nazerigivi *et al*. 2018, Kim *et al*. 2018, Imani *et al*. 2017, Najigivi 2017). However, it has been shown that the mechanical properties of most concretes may be affected by pores shapes. For example, Bubeck *et al*. (2017) experimentally considered the effects of elliptical pores shapes on the failure process and fracture patterns of Brazilian discs of basalt samples. The effect of pore shape on the Brazilian tensile strength of these specimens is also studied by these researchers. They arranged their experimental studies in such a way that the major axes of these elliptical holes are perpendicular to the loading direction.

The novelty of the present work is to study the influence of pore shapes on the concrete strength characteristics, using a bonded particle modelling approach provided by discrete element method (DEM).

2. Numerical modeling

The bonded particle modelling approach used in the two dimensional particle flow code (PFC2D) is based on an explicit discrete element method as originally developed by Cundall 1971 and later on further extended by Potyondy and Cundall 2004. In this modelling technique the samples of rock mass or concretes structure are considered as bonded rigid particles in form of an assembly of circular discs which are connected to one another due to their cohesive and frictional properties. The cohesive and frictional bond are used to provide the element connectivity and the planar walls are assumed to confine the whole specimen.

In this research, the parallel bond model is used to simulate the contact points in between the particles in the assembly. The assigned values of bonding strengths may influence the macro strength and the cracking and failure process during the loading condition of the material samples. A proper friction coefficient is specified for the bonding and is applied as long as the particles remain in contacts in the particle assembly. When the applied normal stress exceeds that of the specified normal tensile strength of the bonding the tensile cracks may be induced while the shear cracks may be generated as the applied shear stress exceed that of the specified shear bonding strength either due to in plane shearing or rotation (out of plane shearing) of the particles. It has been shown that the contact tensile strength may immediately decrease to zero after the breaking of the bonds but shear strength decreases to that of the residual one (Itasca Consulting Group Inc 2004, Cho *et al.* 2007, basic micro-parametric 2008, Potyondy and Cundall 2004, Ghazvinian *et al.* 2012, Sarfarazi *et al.* 2014).

The discrete element code requires only the basic microscopic parameters such as contact forces, bonding stiffness, bonding strength and contact friction to be specified for each particle assembly. However, these parameters are to be adjusted so that the macro scaled mechanical behavior of the modeled material sample can be provided. Therefore, an explicit finite difference scheme is provided in this code to solve the equations of motions (second Newton's law) so that the initiation and propagation of bonding breaks may be tackled through the modelled particle assembly (Potyondy and Cundall 2004).

Table 1 gives a typical values of micro-properties of the particle assembly adopted for calibrating a particular discrete element code

2.1 The micro-properties specified to calibrate the numerical method

Some simple standard tests such as the uniaxial compressive strength (UCS) and the Brazilian tensile strength (BTS) are usually used for calibrating the micro-properties of the particle assembly used in the numerical modeling of the material samples in a particular discrete element code.

2.1.1 Unconfined compressive strength (UCS) test

A model of two moving walls compressing the particle assembly from both sides as illustrated in Fig. 1(a), is used in PFC2D to simulate the compression testing of rock like materials. The solid lines represent the breakage of bonds at the micro cracks locations. Tensile and shear cracks are indicated by black and red lines, respectively. However, this failure process is somewhat similar to that observed experimentally in the laboratory (Fig. 1(a)). These walls are considered as the frictionless rigid plates. The numerically modelled testing specimen have a height 108 mm and width 54 mm. The particle size distribution is normally used for particles in the assembly with particles radii ranging from 0.27 to 0.4212 mm. These particle's radii are chosen such that the computational efficiency of the code increases and also minimizing its running time for the solution of a specific geo-mechanical problem. A reasonable value for a dense packing of particles requires a porosity ratio of 0.08. The appropriate elasticity modulus *E*, the Poisson's ratio

Table 1 micro properties used to represent the intact rock

Parameter	Value
Type of particle	disc
Density (kg/m3)	3500
Minimum radius (mm)	0.27
Size ratio	1.56
Porosity ratio	0.08
Damping coefficient	0.7
Contact young modulus (GPa)	32
Stiffness ratio	2
Parallel bond radius multiplier	1
Young modulus of parallel bond (GPa)	32
Parallel bond stiffness ratio	2
Particle friction coefficient	0.5
Parallel bond normal strength, mean (MPa)	20
Parallel bond normal strength, SD (MPa)	2
Parallel bond shear strength, mean (MPa)	20
Parallel bond shear strength, SD (MPa)	2

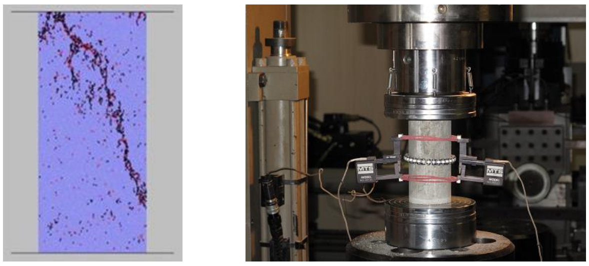

(a) (b)

Fig. 1 (a) the failure pattern in numerical simulation, (b) experimental unconfined compressive test.

Table 2 macro-mechanical properties of model material in experimental tests and PFC2D

Mechanical properties	Experimental results	PFC2D Model results
Elastic modulus (GPa)	33	33
Poisson’s ratio	0.2	0.19
UCS (MPa)	18.3	18
Tensile strength (MPa)	2	4

and the uniaxial compressive strength (UCS) for the particular particle assembly can be obtained by PFC2D (Itasca Consulting Group Inc. 2004, Ghazvinian *et al*. 2012).

The experimentally measured UCS procedure is shown in Fig. 1(b). This figure illustrate that an inclined fracture surface may be generated in the model testing of UCS.

A comparison of numerical results with experimental measurements is presented in Table 2.

2.1.2 Brazilian test

The Brazilian tensile strength (BTS) of the specimen can be determined in a rock mechanics laboratory to calibrate the tensile strength of PFC2D model. The diameter of the Brazilian discs is kept constant (54 mm.) and a total number of 5,615 particles are used in all of the numerical modelling of the testing specimens. The lateral walls are moved toward each other at a constant speed of 0.016 m/s, in order to crush the disc sample and provide the tensile fracturing condition for the modelled specimen. The numerical and experimental tested specimens are shown in Fig. 2(a) and 2(c), respectively. The Brazilian disc testing set up is presented in Fig. 2(b). These figures show that the failure process and fracturing pattern of the numerical simulations and laboratory tests are being well matched with each other. Table 2 compares the numerically estimated tensile strength of the testing specimen with the corresponding measure experimental values.

It should be noted that the parallel bond model of discs or spheres may give a very high tensile strength which may not be well matched with the unconfined compressive strength of a typical hard rock (Potyondy and Cundall 2004). May be on claim for matching the numerical tensile strength with experimental one in this research is that the tensile strength of concrete is sufficiently low.

2.2 Brazilian test simulation consisting various pore shape

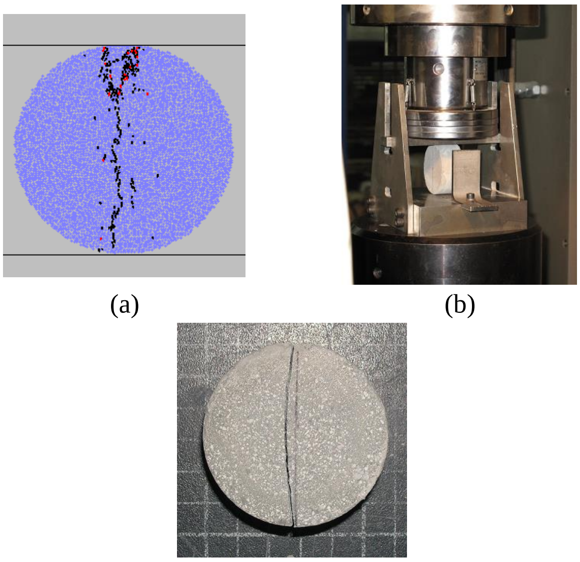

(a) (b) (c)

Fig. 2 the failure pattern in the (a) numerical model, (b) experimental set up, (c) physical samples

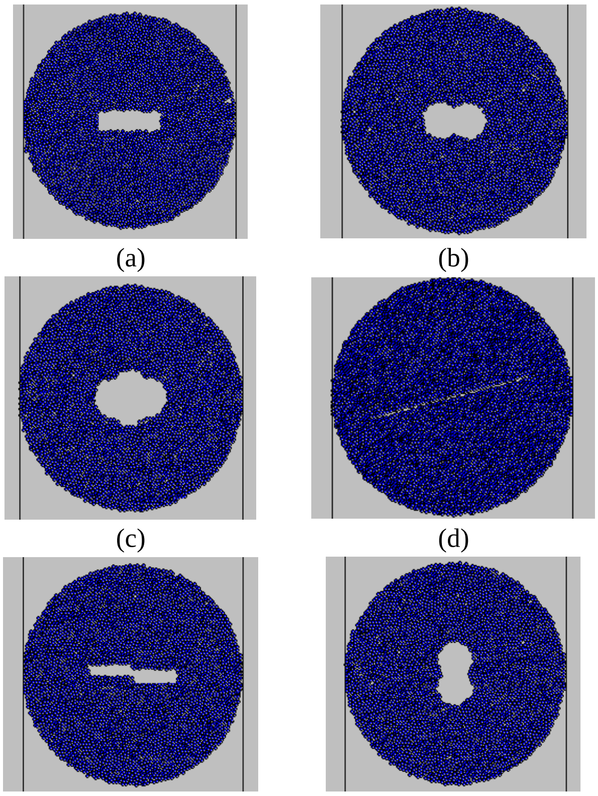

(a) (b) (c) (d) (e) (f)

Fig. 3 Brazilian disc containing various pores shape

The effect of pore shapes on the Brazilian tensile test is then numerically simulated by PFC2D after its calibration. The circular disc models are numerically simulated in PFC2D as shown in Fig. 3. For this simulation process again a Brazilian disc specimen with 54 mm. in diameter containing 5456 circular particles with a minimum radius of 0.27 mm. can be efficiently used. However, the effects of specimen’s boundary and the parameters to minimize the

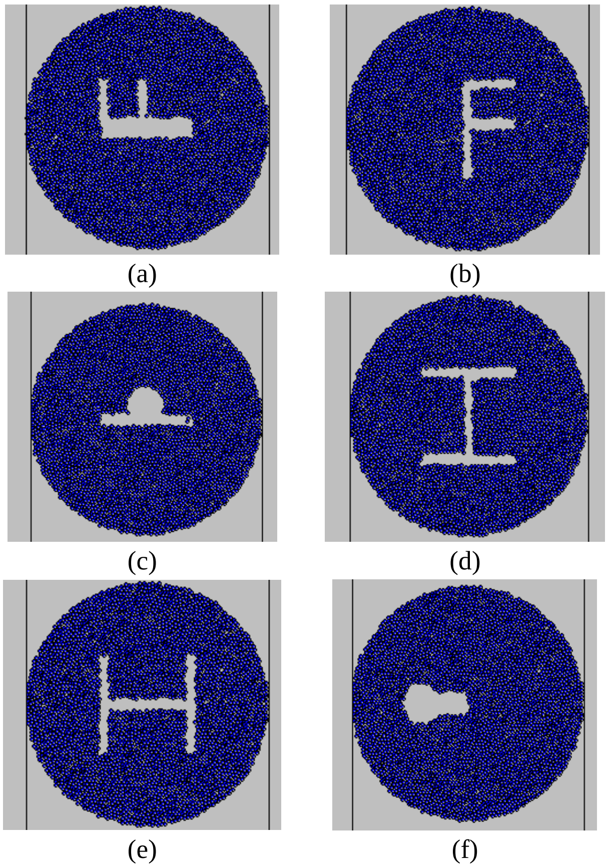

Fig. 3 Continued

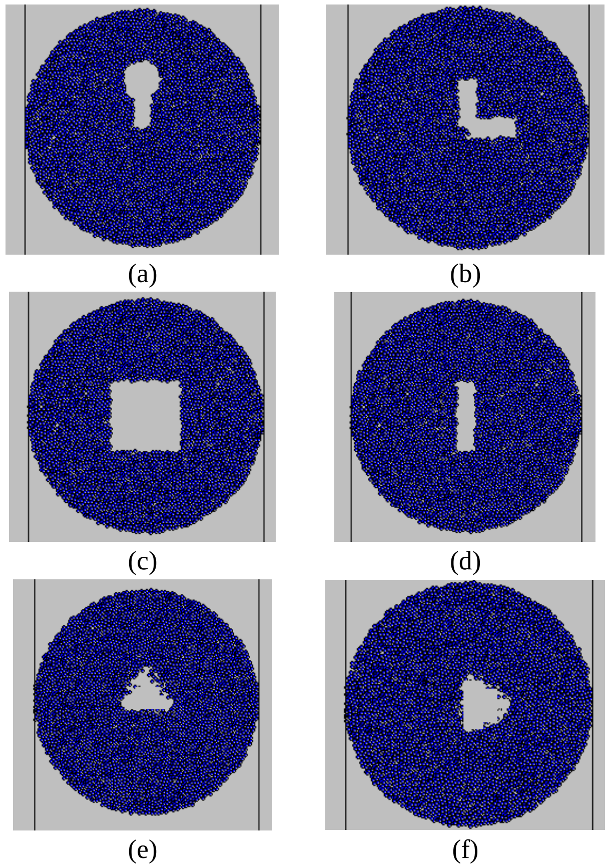

Fig. 3 Continued

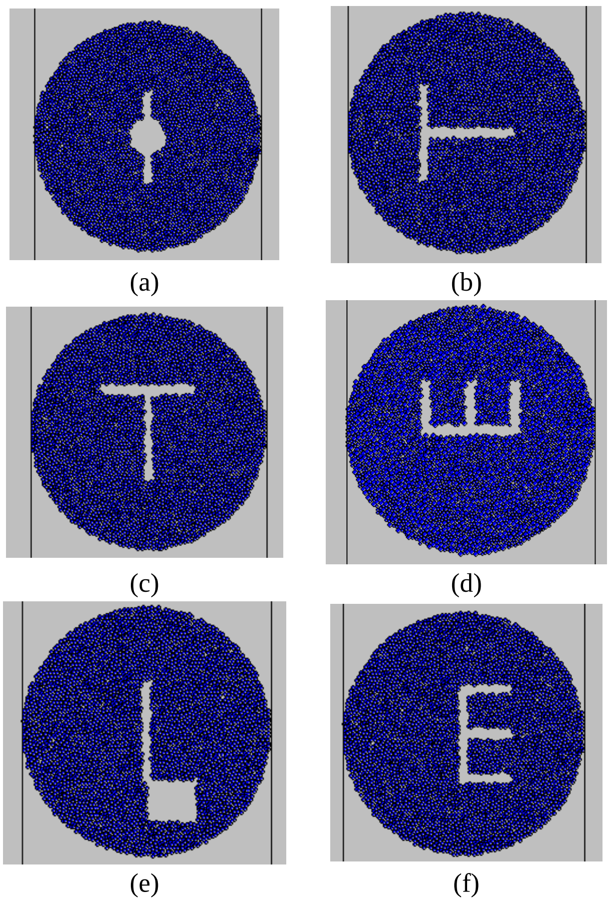

Fig. 3 Continued

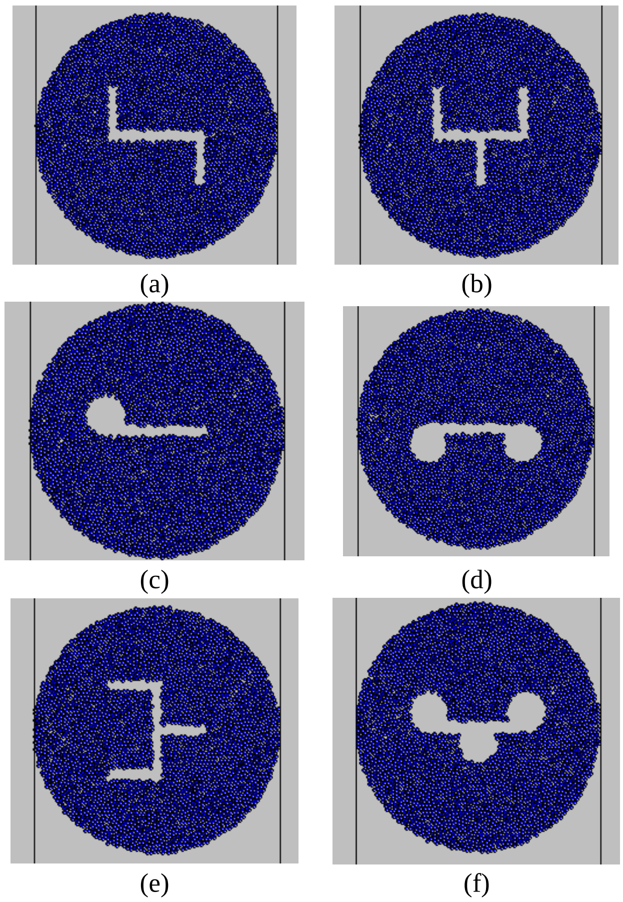

Fig. 3 Continued

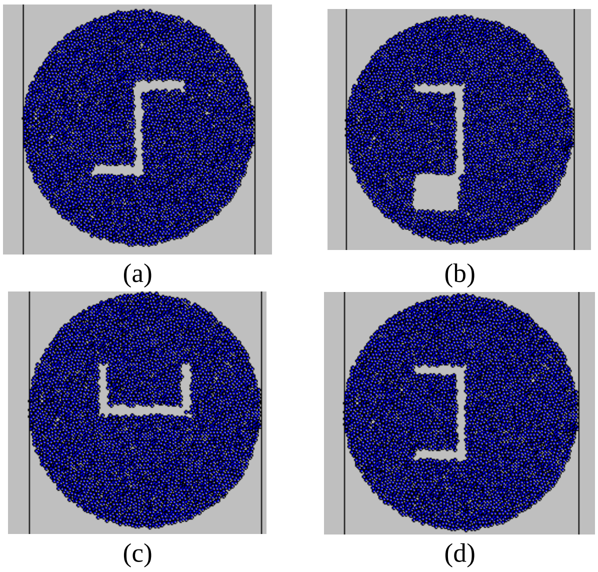

Fig. 3 Continued

running time of the model have been carefully considered in the suggested concrete model size. The porosities with different shape were created in the models. In total, thirty four models containing pores with various shapes were set up to study the influence of pore shapes on failure behavior of numerical models. Two loading wall were situated in the left and right of the models. Left wall moves in *X* direction and right wall moves in opposite side of *X* direction with a constant optimized speed of 0.016 m/s.

3. Results

3.1 Failure process in numerical models:

Figs. 4-9 shows failure pattern in numerical models. Red line and black line represent shear crack and tensile crack, respectively. When pore shape is like Fig. 4(a) and (b), Fig 5(c), (d), (e) and (f), Fig. 6(a) and (d), Fig. 7(b), Fig. 8(b), and Fig. 9(d) two tensile wing crack initiate from left and right of the pore and propagate horizontally till coalescence with model boundary.

When pore shape is like Fig. 4(c) and (e), Fig. 5(a), (c), and (f), Fig. 6(a) and (b), Fig. 8(c) and (d), and Fig. 9(d), three tensile wing crack initiate from left and right of the pore, sometime from lower of the pore, and propagate horizontally till coalescence with model boundary.

When pore shape is like Fig. 4(d) and (f), Fig. 5(b), (d), and (e), Fig. 7(b), (c), (e) and (f), Fig. 8(a), (e) and (f), and Fig. 9(a) and (c), four tensile wing crack initiate from left and right of the pore, sometime from lower and upper of the pore, and propagate till coalescence with model boundary.

From the above findings and results it may be concluded that porosity shape may have an important effect on the failure process of the modeled samples. Whenever larger axis of porosity is perpendicular with loading axis, more cracks develop from the pore. But when the larger axis of porosity is parallel to loading axis, only two or three cracks develop in the model.

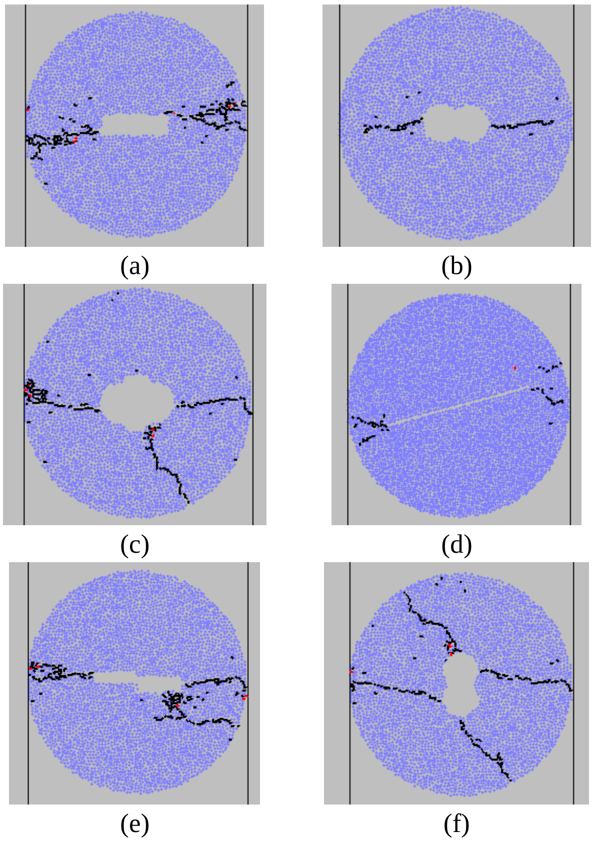

Fig. 4 Failure pattern in Brazilian disc containing various pores shape

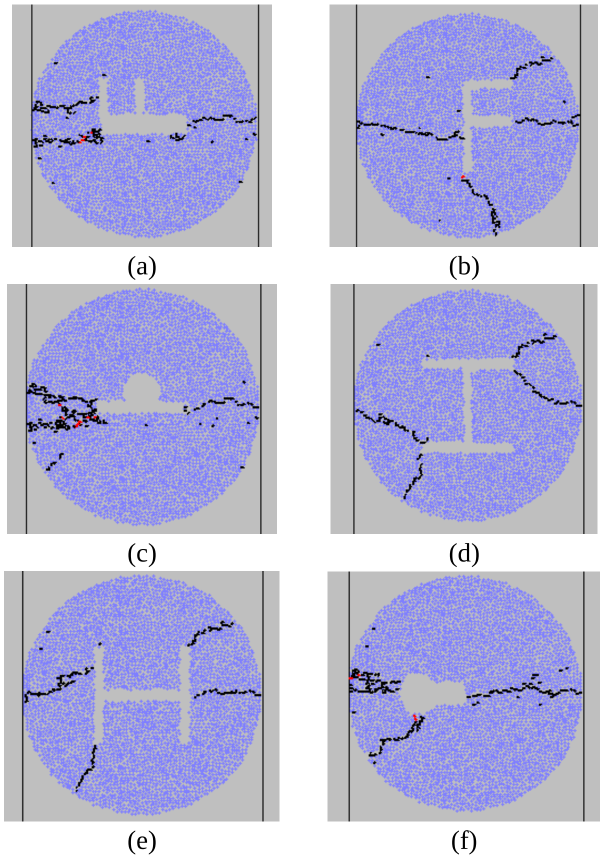

Fig. 5 Failure pattern in Brazilian disc containing various pores shape

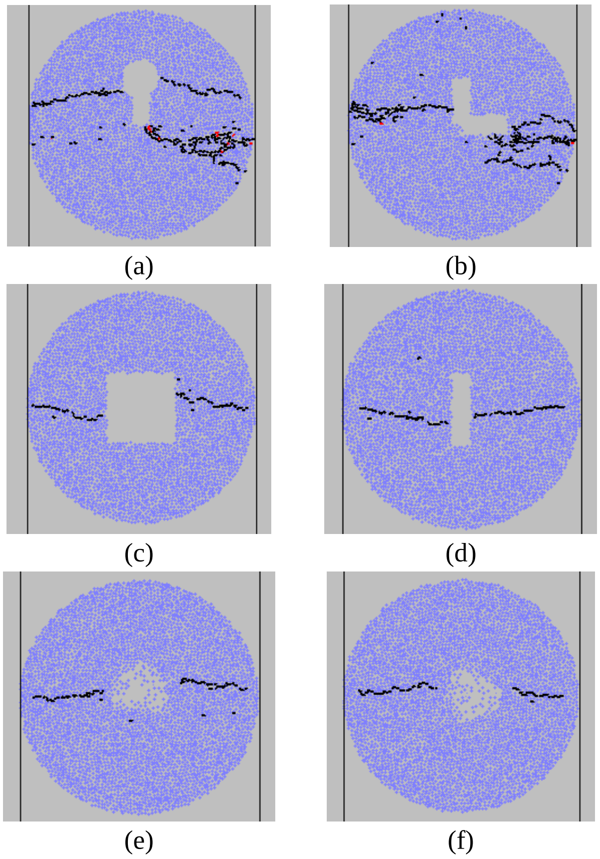

Fig. 6 Failure pattern in Brazilian disc containing various pores shape

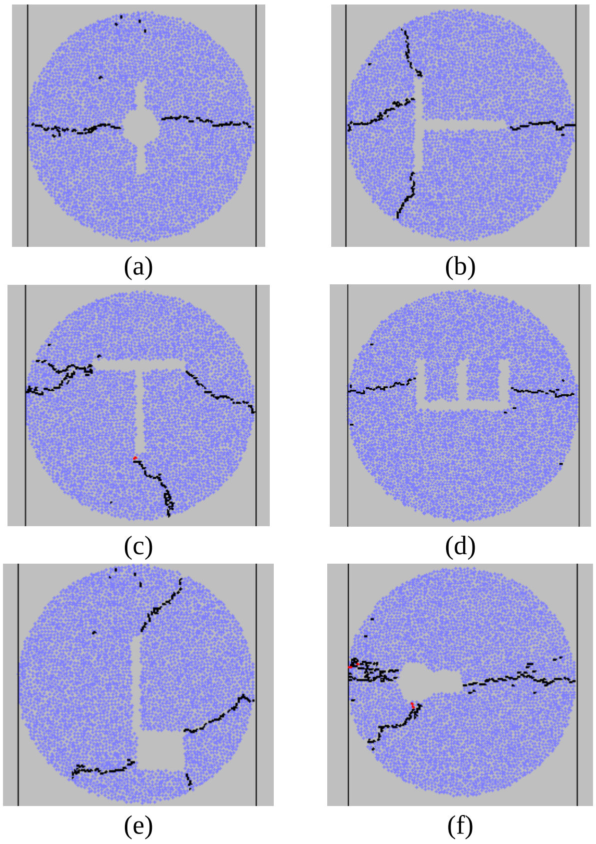

Fig. 7 Failure pattern in Brazilian disc containing various pores shape

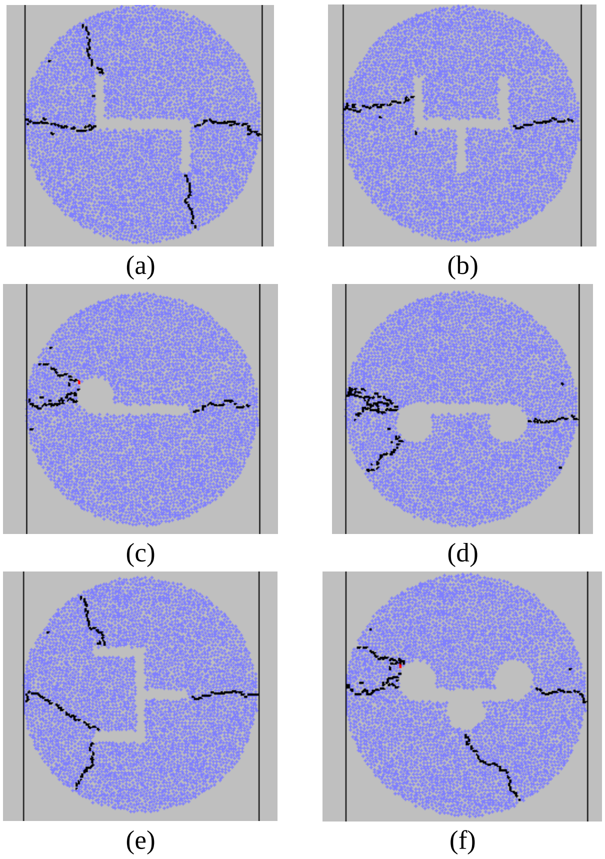

Fig. 8 Failure pattern in Brazilian disc containing various pores shape

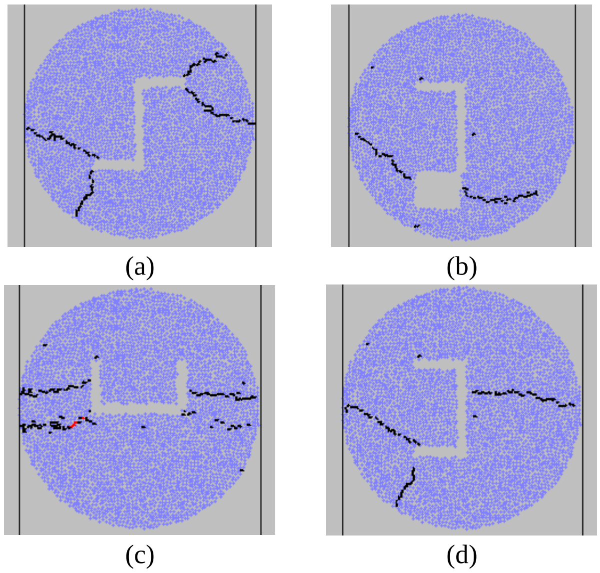

Fig. 9 Failure pattern in Brazilian disc containing various pores shape

3.2 The effect of pore shape on the Brazilian tensile strength:

Fig. 10 shows the effect of pore shape on the tensile strength. As can be seen, the tensile strength has maximum value when larger axis of porosity is perpendicular to loading axis.

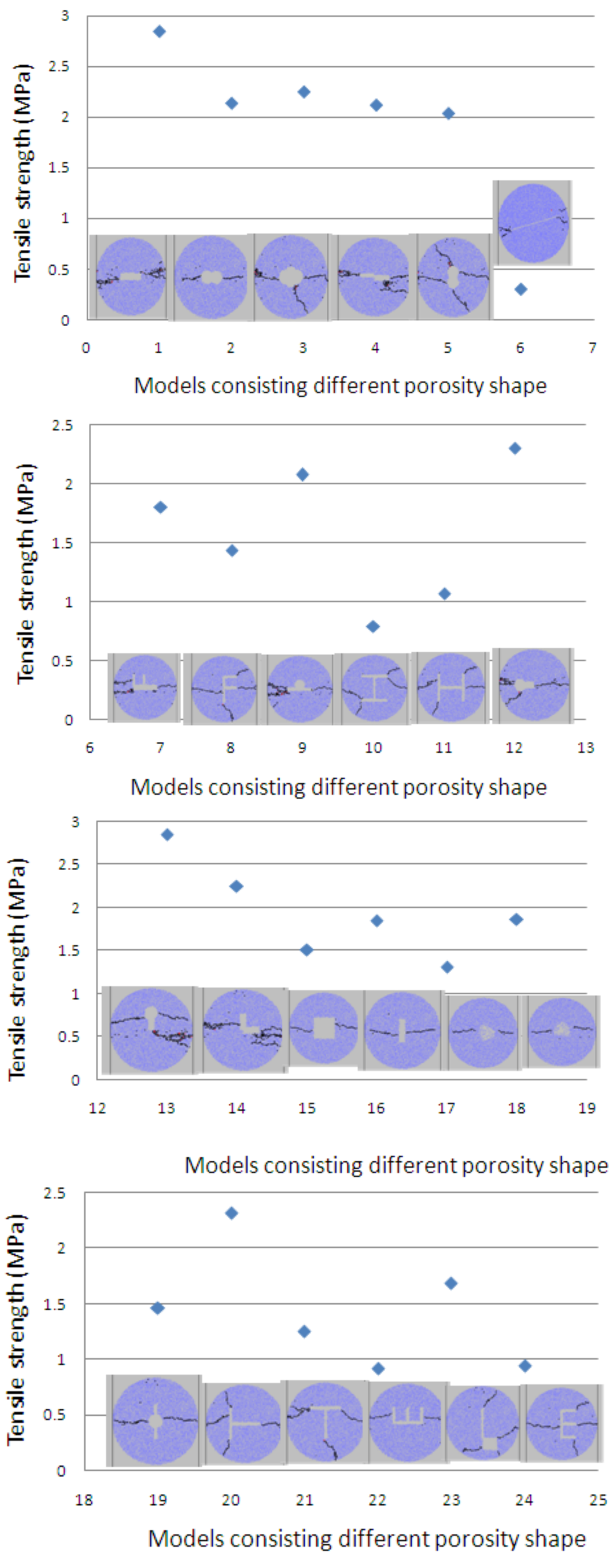

Fig. 10 The effect of pore shapes on the tensile strength

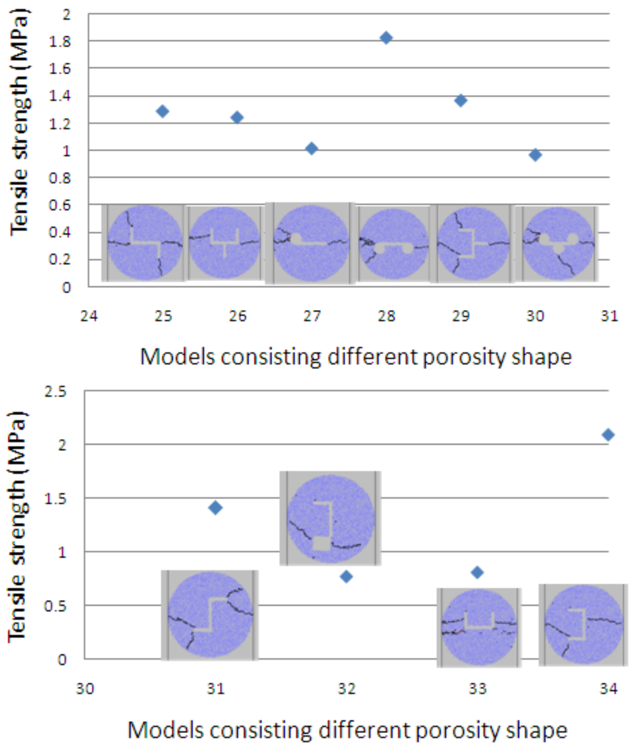

Fig. 10 Continued

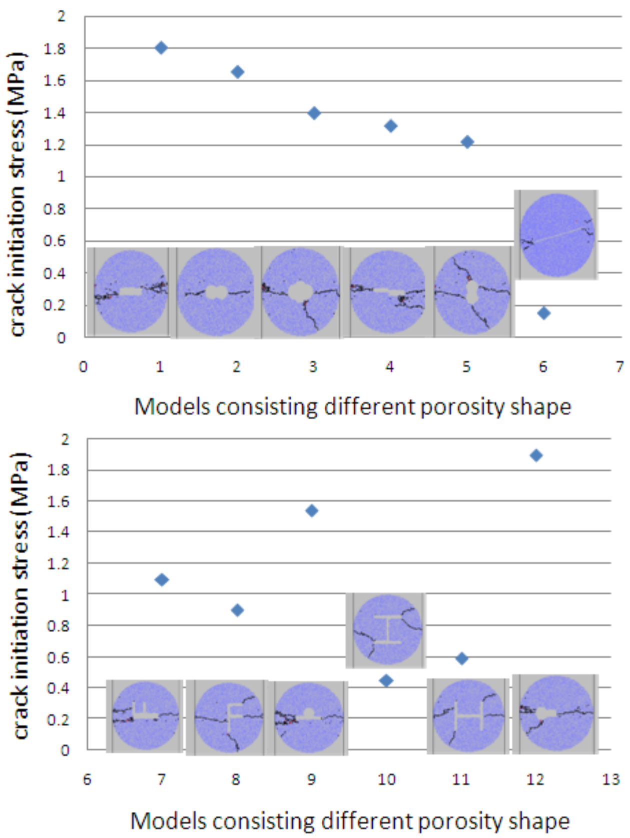

Fig. 11 The effect of pore shape on the crack initiation stress

The discrete of some data are more in Fig. 10; it's due to the effect of porosity shape on strength of material.

3.3 influence of pore shape on the stress field during crack initiation process

The effects of pore shape on the crack initiation stress is shown in Fig. 11. As can be seen, the crack initiation stress has maximum value when larger axis of porosity is perpendicular to loading axis.

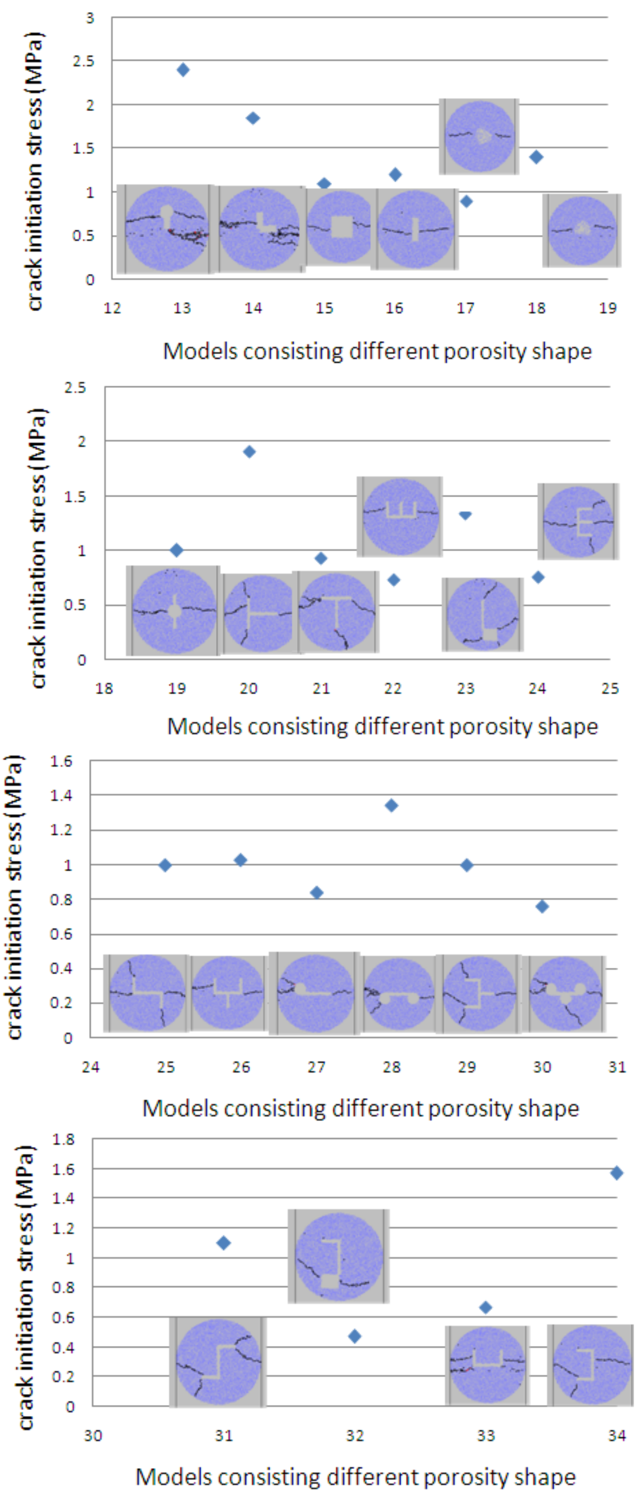

Fig. 11 Continued

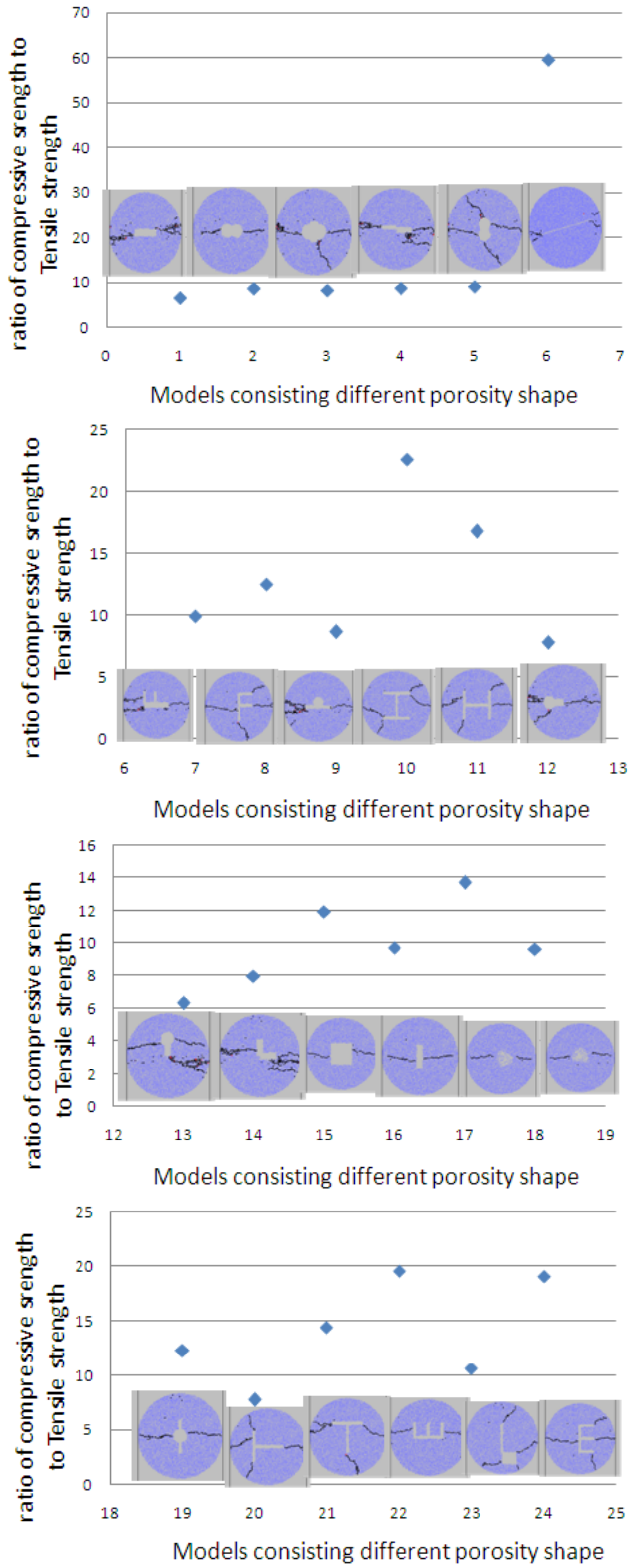

Fig. 12 The effects of porosity shape on the ratio of uniaxial compression strength to tensile strength

3.4 Effects of porosity shape on the ratio of uniaxial compression strength to that of tensile

Fig. 12 shows the effect of porosity shape on the ratio of uniaxial compression strength to the tensile strength of the modelled specimen. As can be seen, the ratio of uniaxial compression strength to that of tensile one has minimum value when larger axis of porosity is parallel to loading axis.

4. Discussion

The porosity shape has important effects on the failure process and Brazilian tensile strength of the concrete. The ratio of uniaxial compression strength to that of tensile one

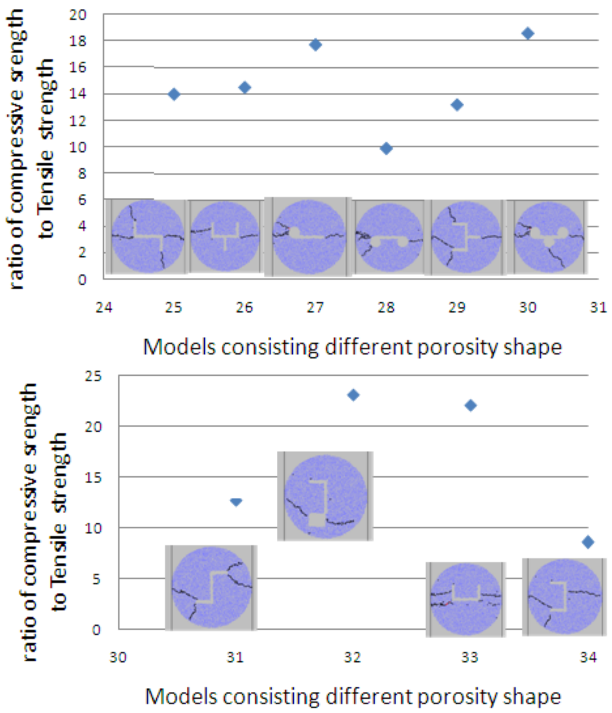

Fig. 12 Continued

of the modelled concrete specimen has minimum value when larger axis of porosity is parallel to loading axis. The crack initiation stress has maximum value when larger axis of porosity is perpendicular to loading axis. Whenever larger axis of porosity is perpendicular with loading axis, more cracks develop from the pore. But when the larger axis of porosity is parallel to loading axis, only two or three cracks develop in the model.

5. Results

In this paper, the effect of porosity shape on concretes tensile strength is studied, using a bonded particle model. Firstly numerical model was calibrated by Brazilian experimental results and uniaxial test out puts. Secondly, Brazilian models consisting various pore shape were simulated and tested (at a constant speed of 0.016 mm/s.).

These modelling results show that

- Porosity shape has important effect on the failure pattern. Whenever larger axis of porosity is perpendicular with loading axis, more cracks develop from the pore.
- The tensile strength has maximum value when larger axis of porosity is perpendicular to loading axis.
- The crack initiation stress has maximum value when larger axis of porosity is perpendicular to loading axis.
- The ratio of uniaxial compression strength to that of tensile one has minimum value when larger axis of porosity is perpendicular to loading axis.

-By PFC2D we can make particle assembly. Its possible to drilled porosity with different shape. Also it's possible to check the cracks initiation, cracks propagation and cracks coalescence in the modelled concrete specimens where previous methods may not be able to predict simultaneously.

References

Al-Harthi, A.A., Al-Amri, R.M. and Shehata, W.M. (1999), "The porosity and engineering properties of vesicular basalt in Saudi Arabia", *Eng. Geol*., **54**, 313-320.

Ashby, M.F. and Sammis, C.G. (1990), "The damage mechanics of brittle solids in compression", *Pure Appl. Geophys*., **133**, 489-521.

Baud, P., Wong, T. and Zhu, W. (2014), "Effects of porosity and crack density on the compressive strength of rocks", *Int. J. Rock Mech. Min. Sci*., **67**, 202-211.

Bourbié, T. and Zinszner, B. (1985), "Hydraulic and acoustic properties as a function of porosity in Fontainebleau Sandstone", *J. Geophys. Res.: Solid Earth*, **90**, 11524-11532.

Bubeck, A., Walker, R.J., Healy, D., Dobbs, M. and Holwell, D.A. (2017), "Pore geometry as a control on rock strength", *Earth Planet. Sci. Lett.*, **457**, 38-48.

Chang, C., Zoback, M.D. and Khaksar, A. (2006), "Empirical relations between rock strength and physical properties in sedimentary rocks", *J. Petrol. Sci. Eng*., **51**, 223-237.

Cho, N., Martin, C.D. and Sego, D.C. (2007), "A clumped particle model for rock", *Int. J. Rock Mech. Min. Sci*., **44**, 997-1010.

Cho, N., Martin, C.D. and Sego, D.C. (2008), "Development of a shear zone in brittle rock subjected to direct shear", *Int. J. Rock Mech. Min. Sci*., **45**, 1335-1346.

Cundall, P. (1971), "A computer model for simulating progressive large scale movements in blocky rock systems", *Proceedings of The Symposium of International Society of Rock Mechanics*, **1**, Nancy, France.

Fan, Y., Zhu, Z., Kang, J. and Fu, Y. (2016), "The mutual effects between two unequal collinear cracks under compression", *Math. Mech. Solid*., **22**, 1205-1218.

Farquharson, J., Heap, M.J., Varley, N.R., Baud, P. and Reuschlé, T. (2015), "Permeability and porosity relationships of edifice-forming andesites: A combined field and laboratory study", *J. Volcanol. Geotherm. Res*., **297**, 52-68.

Ghazvinian, A., Sarfarazi, V., Schubert, W. and Blumel, M. (2012), "A study of the failure mechanism of planar non-persistent open joints using PFC2D", *Rock Mech. Rock Eng*., **45**(5), 677-693.

Haeri, H. (2015), "Propagation mechanism of neighboring cracks in rock-like cylindrical specimens under uniaxial compression", *J. Min. Sci*., **51**(3), 487-496.

Haeri, H. (2016), "Propagation mechanism of neighboring cracks in rock-like cylindrical specimens under uniaxial compression", *J. Min. Sci*., **51**(5), 1062-1106.

Haeri, H. and Sarfarazi, V. (2016), "The effect of non-persistent joints on sliding direction of rock slopes", *Comput. Concrete*, **17**(6), 723-737.

Haeri, H., Khaloo, A. and Marji, M.F. (2015a), "Experimental and numerical simulation of the microcrack coalescence mechanism in rock-like materials", *Strength Mater*., **47**(5), 740-754.

Haeri, H., Khaloo, A. and Marji, M.F. (2015b), "Fracture analyses of different pre-holed concrete specimens under compression", *Acta Mech. Sinica*, **31**(6), 855-870.

Haeri, H., Khaloo, A. and Marji, M.F. (2015c), "A coupled experimental and numerical simulation of rock slope joints behavior", *Arab. J. Geosci*., **8**(9), 7297-7308.

Haeri, H., Sarfarazi, V. and Hedayat, A. (2016a), "Suggesting a new testing device for determination of tensile strength of concrete", *Struct. Eng. Mech*., **60**(6), 939-952.

Haeri, H., Sarfarazi, V. and Lazemi, H. (2016b), "Experimental study of shear behavior of planar non-persistent joint", *Comput. Concrete*, **17**(5), 639-653.

Haeri, H., Sarfarazi, V., Fatehi, M., Hedayat, A. and Zhu, Z. (2016c), "Experimental and numerical study of shear fracture in brittle materials with interference of initial double", *Acta Mech. Soil. Sinica*, **5**, 555-566.

Haeri, H., Shahriar, K. and Marji, M.F. (2013), "Modeling the propagation mechanism of two random micro cracks in rock samples under uniform tensile loading", *Proceedings of the ICF13*.

Haeri, H., Shahriar, K., Fatehi Marji, M. and Moarefvand, P. (2014), "On the crack propagation analysis of rock like Brazilian disc specimens containing cracks under compressive line loading", *Lat. Am. J. Solid Struct*., **11**(8), 1400-1416.

Heap, M.J., Xu, T. and Chen, C. (2014), "The influence of porosity and vesicle size on the brittle strength of volcanic rocks and magma", *Bull. Volcanol*., **76**, 1-15.

Hosseini_Nasab, H. and Fatehi Marji, M. (2007), "A semi-infinite higher-order displacement discontinuity method and its application to the quasistatic analysis of radial cracks produced by blasting", *J. Mech. Mater. Struct*., **2**(3), 439-458.

Imani, M., Nejati, H.R. and Goshtasbi, K. (2017), "Dynamic response and failure mechanism of Brazilian disk specimens at high strain rate", *Soil Dyn. Earthq. Eng*., **100**, 261-269.

Itasca Consulting Group Inc. (2004), Particle Flow Code in 2-Dimensions (PFC2D), Version 3.10, Minneapolis.

Ji, Y., Baud, P., Vajdova, V. and Wong, T.F. (2012), "Characterization of pore geometry of Indiana limestone in relation to mechanical compaction", *Oil Gas Sci. Technol. D'IFP Energ. Nouvelles*. **67**, 753-775.

Ji, Y., Hall, S.A., Baud, P. and Wong, T.F. (2015), "Characterization of pore structure and strain localization in Majella limestone by X-ray computed tomography and digital image correlation", *Geophys. J. Int.*, **200**, 701-719.

Kequan, Y.U. and Lu, Z. (2015), "Influence of softening curves on the residual fracture toughness of post-fire normal-strength mortar", *Comput. Mortar*, **15**(2), 102-111.

Khodayar, A. and Nejati, H.R. (2018), "Effect of thermal-induced microcracks on the failure mechanism of rock specimens", *Comput. Concrete*, **22**(1), 93-100.

Kim, H.M., Lee, J.W., Yazdani, M., Tohidi, E., Nejati, H.R. and Park, E.S. (2018), "E.-S coupled viscous fluid flow and joint deformation analysis for grout injection in a rock joint", *Rock Mech. Rock Eng.*, **51**(2), 627-638.

Lee, S. and Chang, Y. (2015), "Evaluation of RPV according to alternative fracture toughness requirements", *Struct. Eng. Mech.*, **53**(6), 33-46.

Li, S., Wang, H., Li, Y., Li, Q., Zhang, B. and Zhu, H. (2016), "A new mini-grating absolute displacement measuring system for static and dynamic geomechanical model tests", *Measure.*, **82**, 421-431.

Li, S., Wang, H., Li, Y., Li, Q., Zhang, B. and Zhu, H. (2016), "A new mini-grating absolute displacement measuring system for static and dynamic geomechanical model tests", *Measure.*, **82**, 421-431.

Li, Y., Zhou, H., Zhu, W., Li, S. and Liu, J. (2015), "Numerical study on crack propagation in brittle jointed rock mass influenced by fracture water pressure", *Mater.*, **8**(6), 3364-3376.

Liu, X., Nie, Z., Wu, S. and Wang, C. (2015), "Self-monitoring application of conductive asphalt concrete under indirect tensile deformation", *Case Stud. Constr. Mater.*, **3**, 70-77.

Lu, F.Y., Lin, Y.L., Wang, X.Y., Lu, L. and Chen, R. (2015), "A theoretical analysis about the influence of interfacial friction in SHPB tests", *Int. J. Impact Eng.*, **79**, 95-101.

Luquot, L., Hebert, V. and Rodriguez, O. (2016), "Calculating structural and geometrical parameters by laboratory measurements and X-ray microtomography: a comparative study applied to a limestone sample before and after a dissolution experiment", *Solid Earth*, **7**, 441-456.

Ma, T., Wu, B., Fu, J., Zhang, Q. and Chen, P. (2017b), "Fracture pressure prediction for layered formations with anisotropic rock strengths", *J. Nat. Gas Sci. Eng*., **38**, 485-503.

Ma, T., Zhang, Q.B., Chen, P., Yang, C. and Zhao, J. (2017a), "Fracture pressure model for inclined wells in layered formations with anisotropic rock strengths", *J. Petrol. Sci. Eng.*, **149**, 393-408.

Marji, M.F. (2014), "Numerical analysis of quasi-static crack branching in brittle solids by a modified displacement discontinuity method", *Int. J. Solid. Struct.*, **51**(9), 1716-1736.

Marji, M.F., Hosseini-Nasab, H. and Kohsary, A.H. (2007), "A new cubic element formulation of the displacement discontinuity method using three special crack tip elements for crack analysis", *JP J. Solid. Struct*., **1**(1), 61-91.

Mobasher, B., Bakhshi, M. and Barsby, C. (2014), "Backcalculation of residual tensile strength of regular and high performance fibre reinforced concrete from flexural tests", *Constr. Build. Mater.*, **70**, 243-253.

Mohammad, A. (2016), "Statistical flexural toughness modeling of ultra-high performance mortar using response surface method", *Comput. Mortar.*, **17**(4), 33-39.

Najigivi, A., Nazerigivi, A. and Nejati, H.R. (2017), "Contribution of steel fiber as reinforcement to the properties of cement-based concrete: A review", *Comput. Concrete*, **20**(2), 155-164.

Nazerigivi, A., Nejati, H.R., Ghazvinian, A. and Najigivi, A. (2018), "Effects of SiO_2 nanoparticles dispersion on concrete fracture toughness", *Constr. Build. Mater.*, **171**(20), 672-679.

Noel, M. and Soudki, K. (2014), "Estimation of the crack width and deformation of FRP-reinforced concrete flexural members with and without transverse shear reinforcement", *Eng. Struct.*, **59**, 393-398.

Oliveira, H.L. and Leonel, E.D. (2014), "An alternative BEM formulation, based on dipoles of stresses and tangent operator technique, applied to cohesive crack growth modeling", *Eng. Anal. Bound. Elem.*, **41**, 74-82.

Pan, B., Gao, Y. and Zhong, Y. (2014), "Theoretical analysis of overlay resisting crack propagation in old cement mortar pavement", *Struct. Eng. Mech.*, **52**(4), 167-181.

Potyondy, D.O. and Cundall, P.A. (2004), "A bonded-particle model for rock", *Int. J. Rock Mech. Min. Sci*., **41**(8), 1329-1364.

Rajabi, M., Soltani, N. and Eshraghi, I. (2016), "Effects of temperature dependent material properties on mixed mode crack tip parameters of functionally graded materials", *Struct. Eng. Mech.*, **58**(2), 144-156.

Ramadoss, P. and Nagamani, K. (2013), "Stress-strain behavior and toughness of high-performance steel fiber reinforced mortar in compression", *Comput. Mortar*, **11**(2), 55-65.

Rozenbaum, O. and Rolland du Roscat, S. (2014), "Representative elementary volume assessment of three-dimensional x-ray microtomography images of heterogeneous materials, Application to limestones", *Phys. Rev. E*, **89**, 53304,

Sammis, C.G. and Ashby, M.F., (1986), "The failure of brittle porous solids under compressive stress states", *Acta Metall*., **34**, 511-526.

Sarfarazi, V. and Shubert, W. (2016b), "Sliding phenomena in intermittent rock joint", *Periodica Polyechnica Civil Eng.*, **5**, 1-10.

Sarfarazi, V., Faridi, H.R., Haeri, H. and Schubert, W. (2016c), "A new approach for measurement of anisotropic tensile strength of concrete", *Adv. Concrete Constr.*, **3**(4), 269-284.

Sarfarazi, V., Ghazvinian, A., Schubert, W., Blumel, M. and Nejati, H.R. (2014), "Numerical Simulation of the Process of Fracture of Echelon Rock Joints", *Rock Mech. Rock Eng.*, **47**(4), 1355-1371.

Sarfarazi, V., Haeri, H. and Khaloo, A. (2016a), "The effect of non-persistent joints on sliding direction if rock slopes, *Comput. Concerete*, **7**, 723-737.

Schaefer, L.N., Kendrick, J.E., Oommen, T., Lavallée, Y. and Chigna, G. (2015), "Geomechanical rock properties of a basaltic volcano", *Volcanol.*, **3**, 29.

Schmitt, M., Halisch, M., Müller, C. and Fernandes, C.P. (2016), "Classification and quantification of pore shapes in sandstone reservoir rocks with 3-D X-ray micro-computed tomography", *Solid Earth*, **7**, 285-300.

Shuraim, A.B., Aslam, F., Hussain, R. and Alhozaimy, A. (2016), "Analysis of punching shear in high strength RC panels-experiments, comparison with codes and FEM results", *Comput. Concrete*, **17**(6), 739-760.

Simmons, G. and Richter, D. (1976), "Microcracks in rocks", *Chem. Phys. Rock. Min.*, **76**(2), 105-137.

Tiang, Y., Shi, S., Jia, K. and Hu, S. (2015), "Mechanical and dynamic properties of high strength concrete modified with lightweight aggregates presaturated polymer emulsion", *Constr. Build. Mater.*, **93**, 1151-1156.

Tiang, Y., Shi, S., Jia, K. and Hu, S. (2015), "Mechanical and dynamic properties of high strength concrete modified with lightweight aggregates presaturated polymer emulsion", *Constr. Build. Mater.*, **93**, 1151-1156.

Wang, J., Xie, L.Z., Xie, H.P., Ren, L., He, B., Li, C.B., Yang, Z.P. and Gao, C. (2016a), "Effect of layer orientation on acoustic emission characteristics of anisotropic shale in Brazilian tests", *J. Nat. Gas Sci. Eng.*, **36**, 1120-1129.

Wang, Q.Z., Feng, F., Ni, M. and Gou, X.P. (2011), "Measurement of mode I and mode II rock dynamic fracture toughness with cracked straight through flattened Brazilian disc impacted by split Hopkinson pressure bar", *Eng. Fract. Mech.*, **78**(12), 2455-2469.

Wang, X., Zhu, Z., Wang, M., Ying, P., Zhou, L. and Dong, Y. (2017), "Study of rock dynamic fracture toughness by using VB-SCSC specimens under medium-low speed impacts", *Eng. Fract. Mech.*, **181**, 52-64.

Wu, Z.J., Ngai, L. and Wong, Y. (2014), "Investigating the effects of micro-defects on the dynamic properties of rock using Numerical Manifold method", *Constr. Build. Mater.*, **72**, 72-82.

Yaylac, M. (2016), "The investigation crack problem through numerical analysis", *Struct. Eng. Mech.*, **57**(6), 44-60.

Zhang, Q.B. and Zhao, J. (2014), "Quasi-static and dynamic fracture behaviour of rock materials: phenomena and mechanisms", *Int. J. Fract.*, **189**, 1-32.

Zhang, S.W., Shou, K.J., Xian, X.F., Zhou, J.P. and Liu, G.J., (2018), "Fractal characteristics and acoustic emission of anisotropic shale in Brazilian tests", *Tunn. Underg. Space Technol.*, **71**, 298-308.

Zhao, Y., Zhao, G.F. and Jiang, Y. (2013), "Experimental and numerical modelling investigation on fracturing in coal under impact loads", *Int. J. Fract.*, **183**(1), 63-80.

Zhou, J.R., Wei, J., Yang, T.H., Zhu, W.C., Li, L.C. and Zhang, P.H. (2018), "Damage analysis of rock mass coupling joints, water and microseismicity", *Tunn. Underg. Space Technol.*, **71**, 366-381.

Zhu, W., Baud, P., Vinciguerra, S. and Wong, T.F. (2011), "Micromechanics of brittle faulting and cataclastic flow in Alban Hills Tuff", *J. Geophy. Res.: Solid Earth*, **10**(6), 56-70.

CC